C.P. No. 542

C.P. No. 542

MINISTRY OF AVIATION

AERONAUTICAL RESEARCH COUNCIL

CURRENT PAPERS

Pressure Measurements at the Centre of a 40° Swept Back Wing with R.A.E. 101-10 Sections at Zero Incidence and Transonic Speeds

by

J. E. Rossiter

LONDON: HER MAJESTY'S STATIONERY OFFICE

1961

PRICE 4s. 6d. NET

C.P. No. 542

U.D.C. No.533.693.1:533.69.048.2:533.6.011.35

June, 1959

PRESSURE MEASUREMENTS AT THE CENTRE OF A 40° SWEPT BACK WING WITH R.A.E. 101-10 SECTIONS AT ZERO INCIDENCE AND TRANSONIC SPEEDS

by

J.E. Rossiter

SUMMARY

Pressure distributions have been measured on a 40° swept back wing with 10% thick R.A.E. 101 sections in combination with a rectangular section body.

The range of investigation included speeds from M_o = 0.5 to 1.22 at zero wing incidence at a Reynolds number of 1.3 million based on the wing chord. For some of the tests, boundary layer transition was fixed ahead of the 10% chord line on the wing.

Between Mach numbers of 0.88 and 0.94 the pressure distribution in the wing-body junction changed from subsonic to one having the shape associated with the flow at a supersonic free stream Mach number.

At subsonic speeds agreement between the measured pressure distribution in the wing body junctions and an estimate made by the method given by Küchemann and Weber[1] was only fair mainly because the body side does not act as a true reflection plane.

At supersonic speeds, the method given by Bagley for estimating the pressure distribution at the centre section, gives the correct shape for the distribution at Mach numbers as low as 1.02 but the magnitude is in error, particularly over the rear of the section. Agreement between estimated and measured values improves as Mach number is increased but is only fair at the highest test Mach number, M_o = 1.22.

Previously issued as R.A.E. Tech. Note No. Aero.2630 - A.R.C. 21,494

LIST OF CONTENTS

LIST OF ILLUSTRATIONS

LIST OF ILLUSTRATIONS (Contd)

1 INTRODUCTION

One method[1] of designing waisted bodies to reduce the drag of swept-wing body combinations at transonic speeds, requires the calculation of the pressure distribution at the centre of the swept back wing. A method of calculating this pressure distribution for subsonic speeds has been given by Küchemann and Weber[1] and checked experimentally by Bateman and Lawrence[2]. For supersonic speeds, Bagley has suggested a method based on linear theory which is to be verified by tests in the 8 ft × 6 ft Transonic Tunnel on a 55° swept wing with 8% thick R.A.E. 101 sections. This model should have a critical Mach number, away from the centre section, of about 1.2 at zero lift. As however the model was not due to be available until late in 1958, preliminary tests were made on an existing model consisting of a 40° swept wing with 10% thick R.A.E. 101 sections combined with a rectangular section fuselage (see Fig.1). It has been assumed that the pressure distribution at the true centreline will be the same as that measured in the wing body junction (after subtracting a component due to the body nose shape). The errors involved in this assumption are discussed in paragraph 3.3.2.

The critical Mach number for an infinite wing of the same section and sweepback as that of the model is only 0.91 at zero lift. This low value indicates that strong shock waves will be present on the wing at low supersonic speeds, making doubtful the suitability of the model for the investigation. However it was hoped that the results would at least indicate the order of accuracy of Bagley's method.

The model was provided with a large number of pressure holes on the wing surface and, although the principal interest of this investigation is in the junction distribution, pressures were measured at all the available holes. In addition the pressure distribution along the roof of the tunnel was measured, to help in the assessment of tunnel interference (given in the Appendix).

The tests were made in the 8 ft × 6 ft Transonic Tunnel.

2 THE MODEL

2.1 Shape

The principal dimensions of the model are given in Fig.1. The wing has 40° sweepback and 10% thick R.A.E. 101 sections. It has a chord of 13 inches except near the tips and an aspect ratio of 3.68.

The body is of rectangular cross section in the vicinity of the wing and has an elliptically shaped nose.

The model had a maximum cross section area of 48.4 sq in. giving a model/tunnel blockage ratio of 0.7%.

2.2 Construction

The wing was built of compressed wood in two halves, split in the horizontal plane to facilitate the insertion of pressure tubes. The two halves were bonded together and also clamped at the centre section by a steel frame which was in turn bolted to a sting support.

The body is hollow and made, in two parts, from teak. Pressure tubes were led out through a hole in the rear of the body and thence along the sting. In general 3/32 O.D. copper tubing was used for the pressure lines

but for a few pressure holes space limitations made it necessary to use 1 mm O.D. stainless steel tubing.

2.3 Pressure points

Complete chordwise pressure plotting stations (see Fig.1) were provided at stations j and b on the starboard wing and station f on the port wing. These give the detailed distributions at the wing body junction, an intermediate station and a station comparatively free of junction influence, respectively. A few pressure orifices were provided at stations a, c and d on the starboard wing to facilitate the construction of isobar patterns. Station e on the starboard wing, but the same distance from the centreline as section f, was intended as a check on model symmetry.

3 THE TESTS

3.1 The tunnel

This test was one of the first made after the R.A.E. 10' × 7' High Speed Tunnel was converted to the R.A.E. 8' × 6' Transonic Tunnel. The working section has 24 longitudinal slots giving an open area ratio of 11%. The slots start with zero width at Sta -1' 2"*, expand to their full width at Sta 6' 10" and run at constant width from there to Sta 15'. The model sting support is carried on two vertical lead screws running in a fairing which spans the tunnel from roof to floor. The leading edge of the fairing was at the 15' 3" station. The model was mounted in the tunnel with its nose at station 6' 10.7". During the test the roof and floor were each diverged 0.22°.

3.2 Range of investigation

The test was made at zero incidence, at a Reynolds number of approximately 1.3 million based on the wing chord, and through a Mach number range from 0.5 to 1.22.

The test was made in three runs as detailed below:-

Run No.	B.L. transition	Pressures measured at
1	Natural	Stations a, c, d, f, j (U/S)
2	Natural	Stations b, e, j (L/S) tunnel roof
3	Fixed	Stations f and j

The test with natural transition was made in two runs because the number of pressure holes exceeded the manometer capacity.

Transition was fixed (on the wing only) by distributed roughness ahead of the 10% chord line, on both surfaces. The roughness was achieved by a mixture of carborundum powder in aluminium paint applied to the wing surface by means of a small roller. The grain size of the carborundum powder was about 0.003 inches.

---

* Longitudinal stations in the working section are measured from a structural datum.

3.3 Accuracy

3.3.1 Tunnel Mach number M_o

Tunnel Mach number M_o is defined as the mean Mach number in the empty working section and has been related to the ratio of plenum chamber pressure to total head pressure by previous calibration using a centreline static tube. The variation of Mach number over the empty working section was within ±0.001, ±0.002 and ±0.004 of the mean for Mach numbers of 0.5, 1.0 and 1.2 respectively. The tunnel Mach number was held within ±0.002 of its nominal value during these tests.

3.3.2 C_p and local Mach number

The variation in Mach number in the empty working section corresponds to variation in C_p of ±0.005, ±0.003 and ±0.007 at Mach numbers of 0.5, 1.0 and 1.2 respectively.

In relating the junction measurements to those at the centre of a swept-back wing there are two additional sources of error. One is introduced by the pressure measuring holes being positioned slightly away from the junction and the other by the imperfection of the fuselage as a reflecting surface. An idea of the magnitude of these errors can be obtained from Ref.2 where Bateman and Lawrence compare their measurements at the centre of a 12% thick 40° swept wing with Hartley's[3] in the junction of a similar wing and a rectangular section fuselage. At Mach numbers of 0.5, 0.82 and 0.86 and at about 50% chord the pressure coefficients measured in the wing body junction were 0.03, 0.06 and 0.06, respectively, higher than those measured at the true centre section. The difference between the pressure coefficients measured on the two configurations decreased toward the leading and trailing edges. At M_o = 0.90 the pressure coefficient in the junction at 50% chord was only 0.02 higher than that measured at the true centre section, but whereas the shockwave at the true centre section had reached the wing trailing edge that in the junction had not. Thus it may be anticipated that at subsonic speeds values of the pressure coefficient in the junction will be rather higher than those at the true centre section and that at transonic speeds conditions at the rear of the section may be in error.

3.4 Wall interference

The question of wall interference on the measured pressure is discussed in the Appendix. It would appear that pressures measured at sections b and j between $M_o \div 1.05$ and 1.2 and at section f above $M_o \div 1.05$ are certainly invalid and have therefore been omitted from the general discussion. They may, however, be seen in Figs.18 to 20. Measurements made between M_o = 1 and 1.05 have been included but should be treated with caution. The results presented for sections b and j above M_o = 1.2 are thought to be slightly in error near the trailing edge (see Appendix).

4 RESULTS

The pressure distributions measured on the upper and lower wing surfaces agree well with each other up to the critical Mach number. At higher speeds, different pressures were measured on the two surfaces and in particular the shockwaves formed at different positions. It is thought that these differences were due to small errors in the wing profile and in the condition of the pressure holes. Because of the different shockwave positions it is unrepresentative to take a mean of the upper and lower surface pressures. Examination of the model showed that the pressure holes on the upper wing surface were in better condition than those on the lower

surface and the upper surface pressure distributions are smoother, so results have been presented for this surface only.

Fixing boundary layer transition had no significant effect on the pressure distributions at section j, presumably because the boundary layer was already turbulent in the junction. However the pressure distribution at section f was affected (see Fig.2). With transition fixed, up to M = 0.909, the shockwave forms further forward than where transition occurs naturally. At higher speeds the shockwave is not so well defined when transition is fixed. It is thought that the pressure distributions obtained with boundary layer transition fixed are less likely to have been affected by shockwave boundary layer interaction and so results presented for sections f and j are with boundary layer transition fixed. The results presented for section b are with transition occurring naturally, in the absence of any results for transition fixed. The isobar patterns of Fig.15 were constructed from the results with transition occurring naturally, for consistency at the various stations.

5 DISCUSSION

5.1 The centre section (section j)

5.1.1 Development of flow

The distributions of local Mach number in the wing body junction for various tunnel Mach numbers are shown in Fig.3 and in Fig.4 the local Mach number has been plotted against tunnel Mach number for various chordwise stations.

The flow in the junction is subsonic for tunnel Mach numbers below 0.86, but by 0.88 a small supersonic region has developed. This supersonic region extends rapidly forward (see Fig.5) and rearward as Mach number is increased over 0.88. Above a Mach number of 0.9 it is terminated by a well defined shockwave which is very close to the trailing edge by a Mach number of 0.94. The rapid fall in trailing edge pressure coefficient (see Fig.6) at a Mach number of about 0.92 probably indicates that the boundary layer has separated behind this shockwave.

The magnitude and position of the peak in the local Mach number distribution are given in Figs.7 and 8 respectively where they are compared with sections on the wing. It is noticeable that for the junction the peak is both smaller in magnitude and further aft than the other sections.

5.1.2 Comparison with estimates

In making an estimate of the pressure distribution in the wing body junction it has been assumed that the body side acts as a reflecting surface so that the pressures are the sum of those at the centre of a wing of the same section and sweepback and that due to the body nose shape.

The pressures at the centre of a swept back wing have been estimated by the method of Küchemann and Weber[1] for subsonic speeds and that due to Bagley for supersonic speeds. The contribution from the body nose shape has been estimated by assuming a source distribution on the body centreline of strength proportional to the rate of change of area and calculating the pressures on a cylinder equal in diameter to the body width. At subsonic speeds a correction has been made for compressibility based on the $(1 - M^2)^{\frac{1}{4}}$ law. For supersonic speeds the method of Warren and Fraenkel[4] has been used. This method gives an answer which is independent of Mach number for points well downstream of the nose. The estimates of the body nose shape contribution to the junction velocity distribution are shown in Fig.9.

Comparison between the estimates and measured pressures is made in Fig.10 for subsonic speeds. Agreement is tolerably good at $M_o = 0.5$ and although the magnitude of the suction is overestimated its position is correct. By $M_o = 0.839$ however both magnitude and position of the suction peak are incorrectly estimated and this state of affairs gets progressively worse up to $M_o = 0.880$. However, most of the difference in magnitude can be accounted for by the experimentally observed differences (noted in para. 3.2.2) between measurements made at the body side and at the true centreline, leaving only an error in the estimation of the position of the Mach number peak.

Even at speeds as high as $M_o = 0.908$ when there is a shockwave on the wing agreement is still good toward the rear of the section. This helps to confirm the hypothesis that the pressures behind a shockwave is unaffected by the presence of the shockwave provided boundary layer separation is absent. By $M_o = 0.930$ the shockwave is almost at the trailing edge and agreement between estimated and measured values breaks down completely.

Comparison between estimated and measured pressure distributions for supersonic speeds are given in Fig.11. The overall shape of the distribution has been well estimated by linear theory for Mach numbers as low as 1.018. However, magnitudes, particularly over the rear of the section, are grossly in error. Agreement between estimated and measured values improve as Mach number is increased but is not good even at the highest test Mach number. It is thought that the discrepancies are caused in the main by the mixed nature of the flow over the wing. Smaller errors are probably caused by boundary layer growth and the fact that the measurements were made in a wing body junction and not at the true centre section.

5.2 Sheared wing section (section f)

The pressure plotting station at section f is sufficiently far from the junction to be only slightly affected by it so that conditions will be very nearly those on a sheared wing of the same section and sweep.

The local Mach number distributions are shown in Fig.12 for a range of free stream Mach numbers, and pressure distributions are compared in Fig.13 with estimates based on reference 1. Up to $M_o = 0.88$ agreement with the estimates is quite good. At $M_o = 0.908$ a strong shockwave forms which moves slowly toward the trailing edge with increase in Mach number. It is of interest to note that the distribution at the rear of the section is still in reasonably good agreement with the estimate at $M_o = 0.908$ even although there is a shockwave on the wing.

5.3 Section b

The local Mach number distribution for section b is shown in Fig.14. The flow becomes sonic locally at a Mach number of 0.83 but there is no evidence of a shockwave on the wing until $M_o = 0.89$. This shock moves rapidly toward the trailing edge of the wing as Mach number is increased and is only just ahead of the trailing edge by $M_o = 0.95$. The peak in the local Mach number distribution is stationary with Mach number at about 33% chord (unlike the junction where the peak moves rearward with increase in Mach number). At supercritical speeds the peak is followed by a gradual fall in Mach number before the main shock is reached. It is possible that this fall in local Mach number is a result of a boundary layer separation caused by a weak shockwave at about 35% chord. There is some evidence, in the photographs given by Bateman and Lawrence[2], that such a shockwave may occur on wings of about this thickness and sweepback.

5.4 Isobar patterns

Isobar patterns for four Mach numbers have been drawn in Fig.15. The isobars have been labelled with values of local Mach number rather

than pressure coefficient so that regions of supersonic flow may be more easily identified.

At $M_o \approx 0.7$ the isobars are straight and approximately parallel to the wing sweep over most of the wing except in the junction. As speed is increased to $M_o \approx 0.88$ the spanwise influence of the junction increases and the isobars over an appreciable area of the wing have either reduced or negative sweep. By $M_o \approx 0.94$, when the shock has reached the trailing edge in the junction, the isobar sweep is reduced over most of the wing. However as speed is further increased, the shockwave moves rearward on the outer sections and the isobar sweep is restored. It will be noted that the position of the peak Mach number moves progressively outboard so that by $M_o \approx 1.05$ it is about one wing chord from the body centreline.

6 APPLICATION TO WING BODY JUNCTION DESIGN

This investigation was undertaken to provide information on the variation of the "centre effect" on swept back wings at transonic speeds in connection with the design of waisted body wing combinations. The principal interest is in checking Bagley's method for calculating the velocity distribution at the centre of a swept back wing.

The comparison with Bagley's estimates in Fig.11, although not good is encouraging, particularly so in view of the low critical Mach number of the model. Assuming, however, that for a wing with a higher critical Mach number, the estimate is no nearer the actual distribution than in the present tests, it is thought that any errors in body waisting which this will introduce will be commensurate with other errors introduced by inadequacies in the basic assumptions of the design method. The over estimation of the junction velocity at the rear of the section will result in waisted shapes with larger bulges near the trailing edge than are necessary, but in a practical case, at least, the size of such bulges may well be limited by other considerations.

7 CONCLUSIONS

1 The flow in the wing body junction was shock free up to $M_o = 0.88$. A shockwave formed on the wing above this speed and moved rapidly toward the trailing edge at the junction.

2 Measured values for the pressure distribution in the junction agree tolerably well with estimates based on the method of Küchemann and Weber[1] up to $M_o = 0.88$. The error in magnitude is about the same as that observed by Bateman and Lawrence[2] for the difference between measurements at a centre section and measurements at a body side, emphasizing that the body does not act as a true reflection plane.

3 Linear theory overestimates the pressure coefficient toward the rear of the junction at supersonic speeds; for this particular model the error is 0.125 at $M_o = 1.018$ decreasing to about 0.06 at $M_o = 1.22$. Agreement over the first 30% of the section is fairly good.

4 For a section where conditions were almost those on an infinite sheared wing, agreement between measured pressures and estimates based on the method of Küchemann and Weber[1] were good up to $M_o = 0.88$. At $M_o = 0.908$ a shockwave was present on the wing but agreement was still good away from the shockwave.

LIST OF SYMBOLS

c	wing chord
C_p	pressure coefficient
C_p^*	pressure coefficient at which speed is sonic
H	tunnel height
M_L	local Mach number
M_o	tunnel Mach number
x	distance measured from leading edge of local chord.

LIST OF REFERENCES

Ref. No.	Author	Title, etc
1	Küchemann, D. Weber, J.	The subsonic flow past swept wings at zero lift without and with body. A.R.C. R. & M. 2908. March, 1953.
2	Bateman, T.E.B. Lawrence, A.J.	Experimental investigation of the pressure distribution at the centre section of a swept back wing at high subsonic speeds. A.R.C. C.P.367. August, 1955.
3	Hartley, D.E.	Investigation at high subsonic speeds of wing fuselage intersection shapes for swept back wings. Part II Pressure measurements on some initial designs. A.R.C. 16,780, December, 1953.
4	Warren, C.H.E. Fraenkel, L.E.	A combination of the quasi-cylindrical and slender body theories. J.R.Ae.Soc. Vol.59 No.532, April, 1955.
5	O'Hara, F. Squire, L.C. Haines, A.B.	An investigation of interference effects on similar models of different size in various transonic tunnels in the U.K. ARA Wind Tunnel Note 27. A.R.C. 21,094. February, 1959.

APPENDIX

TUNNEL WALL INTERFERENCE EFFECTS

1 SUBSONIC SPEEDS

Little is known of the effects of wall constraint on pressure distribution measurements in a slotted tunnel at subsonic speeds. However Ref.5 suggests that such effects are small except for Mach numbers close to unity (> 0.98) for models with a blockage ratio similar to the one of these tests.

2 SUPERSONIC SPEEDS

At supersonic speeds, compression and expansion waves emanating from the model may be reflected from the tunnel walls. Unless these reflected waves are weak or pass well behind the model, results from the test cannot represent a free stream condition. Fig.16 shows the local Mach number distribution along the centre slat of the tunnel roof which was measured during the test. Regions of compression waves coming from the body nose and the wing leading and trailing edges are clearly seen as are the regions of expansion waves coming from the body nose and the wing. It may be anticipated that such a distribution, reflected from the tunnel roof and floor and moved downstream by about $H/2\ (M_o^2 - 1)^{\frac{1}{2}}$ will be superposed on that due to the model at the tunnel centreline. In addition, a similar distribution from the sidewalls will be superposed at the centreline. The superposing of reflections from both roof, floor and sidewalls makes it difficult to trace the wave system in a rectangular tunnel except for the one striking the model furthest upstream, that is the reflection of the body bow wave in the tunnel roof and floor. Fig.18, which gives the local Mach number distribution in the model wing-body junction for some supersonic speeds, shows this bow wave reflection quite clearly; for example at $M_o = 1.161$ it is at about 50% chord and at $M_o = 1.178$ it is at about 85% chord. It is easier to trace the passage of the reflected wave across the model in the cross plots of Fig.4. There, the reflected wave gives a dip in the graph of local Mach number variation with free stream Mach number. For example the wave crosses the 20% chord position at $M_o = 1.14$ and the 50% chord position at $M_o = 1.16$. In Fig.17 the position of the bow shock at the tunnel roof and its reflection at the tunnel centreline are plotted against free stream Mach number. Also plotted in Fig.17 is the position at which the reflected wave would meet the centreline if it were propogated at the free stream Mach angle.

So far in assessing the effect of these reflections, the upstream influence of the bow shock at the tunnel wall and its reflection at the model have been ignored. The extent of the upstream influence at the wall can be seen from Fig.16 and has been plotted in Fig.17. If it is assumed that the extent of the upstream influence will be the same at the model then the interference boundary is as shown in Fig.17.

Hence the pressure measurements in the wing body junction are not free of interference until $M_o = 1.22$ but are only slightly in error at the wing trailing edge above $M_o = 1.2$. As the wing is swept back it must be assumed that sections out on the wing will not be free of interference until higher Mach numbers.

As free stream Mach number decreases, the reflected waves become much weaker and more difficult to trace. It is to be hoped that for speeds just above unity the reflected waves are so weak that they can be ignored. However in Fig.4 a fall followed by a sharp rise in the local Mach number at the rear of the section for $M_o \doteqdot 1.06$ may be due to a reflection of

the wing bow wave and expansion waves from near the wing leading edge. The passage of these waves forward over the model with decreasing Mach number cannot be reliably traced much ahead of 30% chord. As the local Mach number on the wing surface is less than unity ahead of $x/c \div 0.2$ for $M_o = 1.05$. In view of the uncertainity it has been assumed, for the present, that results between $M_o = 1.0$ and 1.05 are not much in error but they should be treated with caution.

Summarising pressures measured at section j (and possibly b) are in general acceptable except between $M_o = 1.05$ and 1.2 and at section f for M_o less than 1.05. These results have been presented in the main body of this Note. The results which are suspect as suffering from tunnel interference are presented in Figs.18 to 20.

WT.2078.C.P.542.K.3 - Printed in England

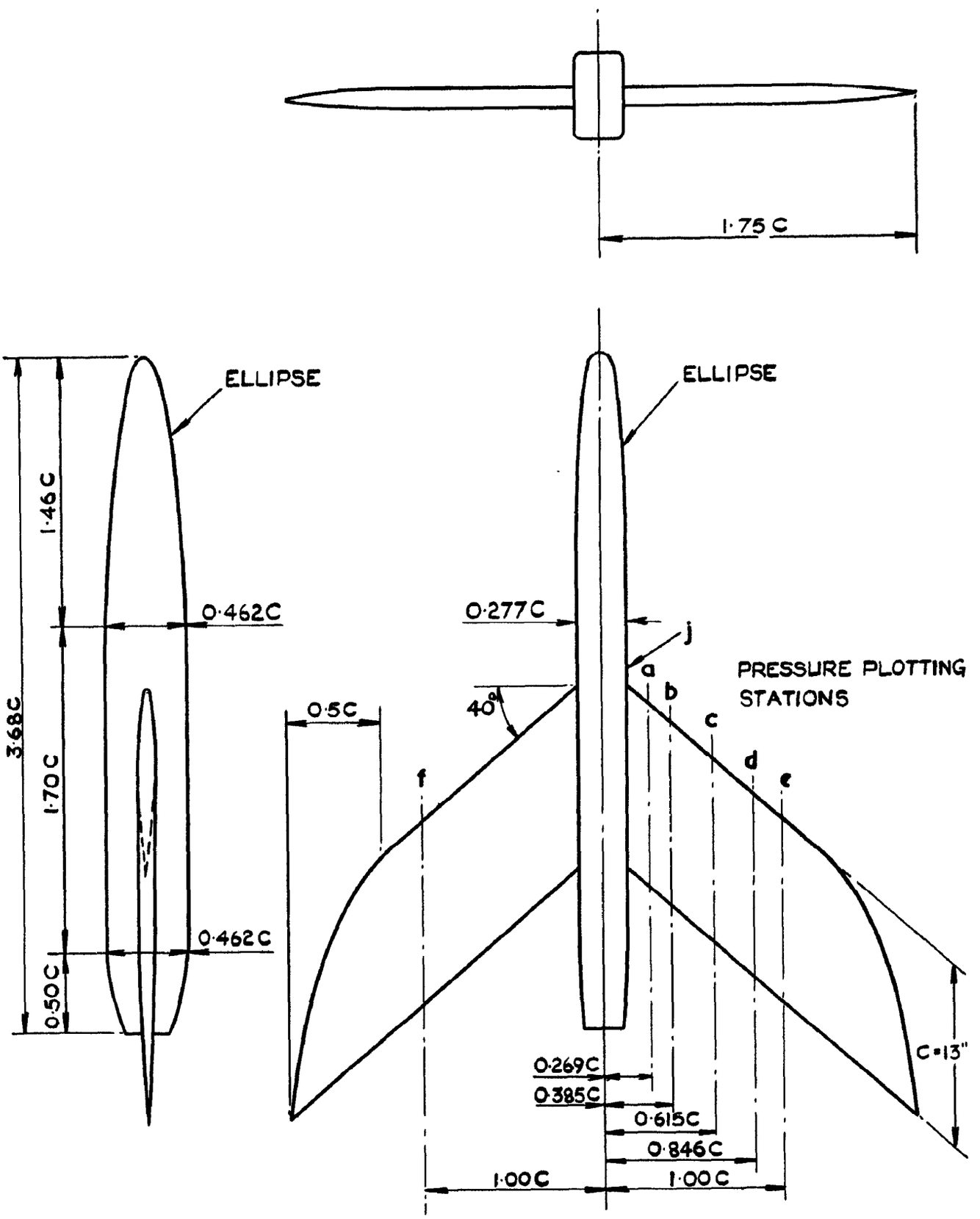

FIG. 1. MODEL GEOMETRY AND POSITION OF PRESSURE PLOTTING STATIONS.

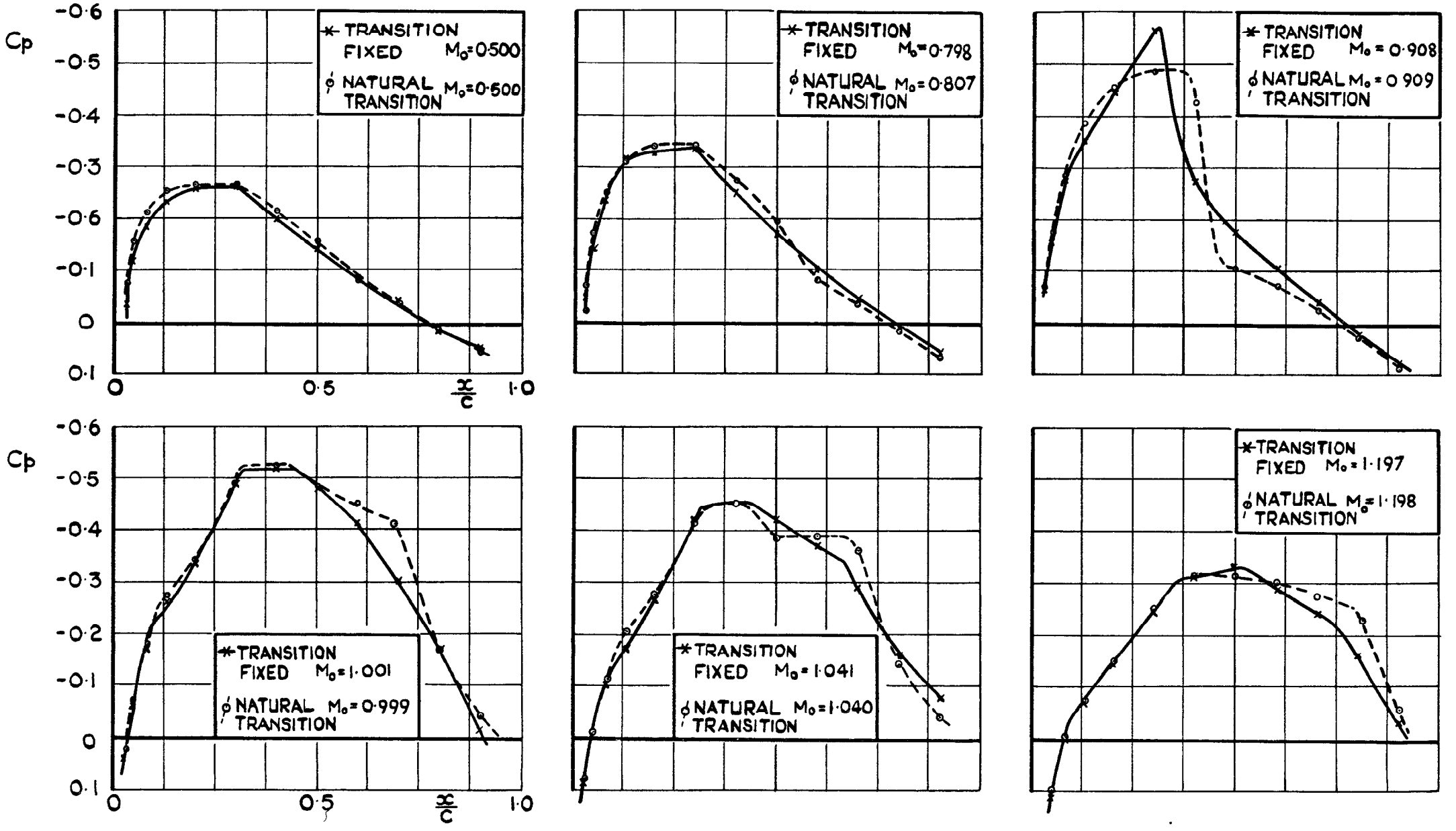

FIG. 2. COMPARISON BETWEEN PRESSURE DISTRIBUTIONS WITH NATURAL AND FIXED TRANSITION SECT f (SEE PARA 4).

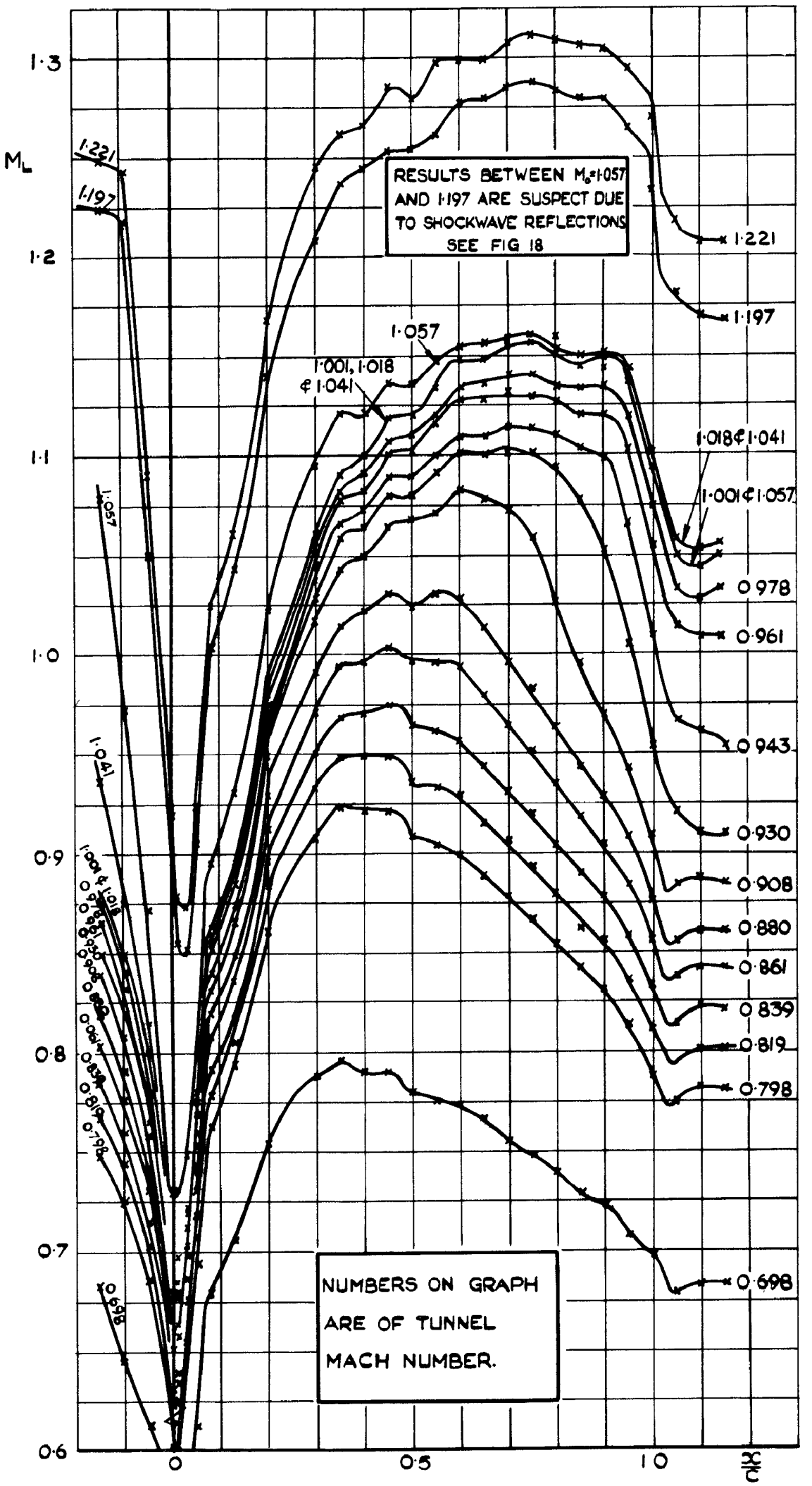

FIG. 3. LOCAL MACH NUMBER DISTRIBUTION IN WING BODY JUNCTION. TRANSITION FIXED. (SEE PARA. 5)

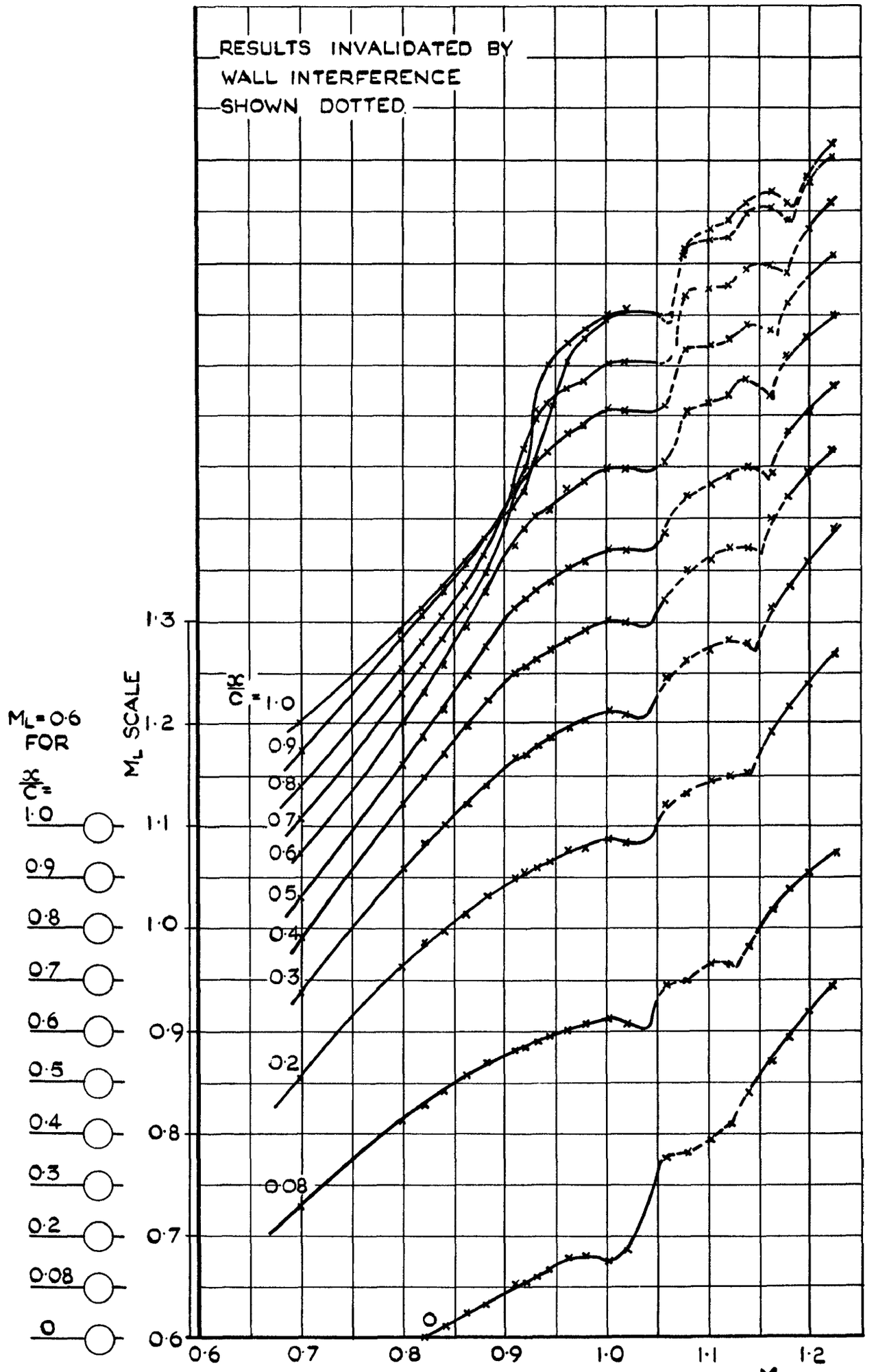

FIG. 4. VARIATION OF LOCAL MACH NUMBER IN WING BODY JUNCTION WITH TUNNEL MACH NUMBER TRANSITION FIXED. SEE (PARA. 5)

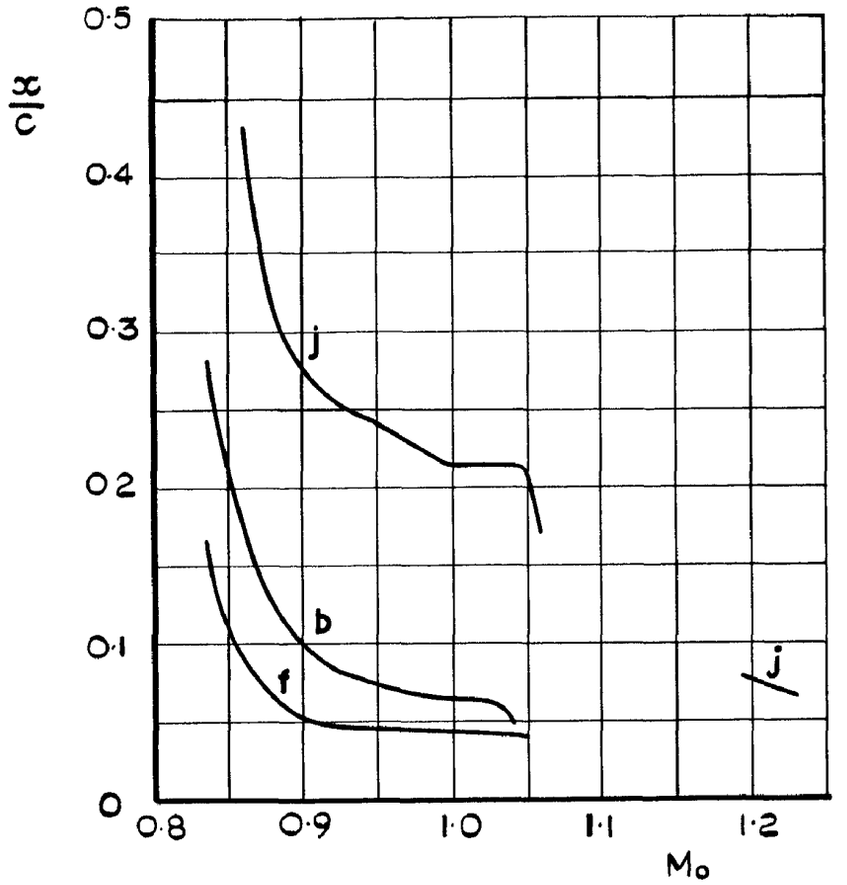

FIG. 5. POSITION OF FORWARD BOUNDARY OF SUPERSONIC REGION AT SECTIONS b,f AND j. (SEE PARA. 5.1)

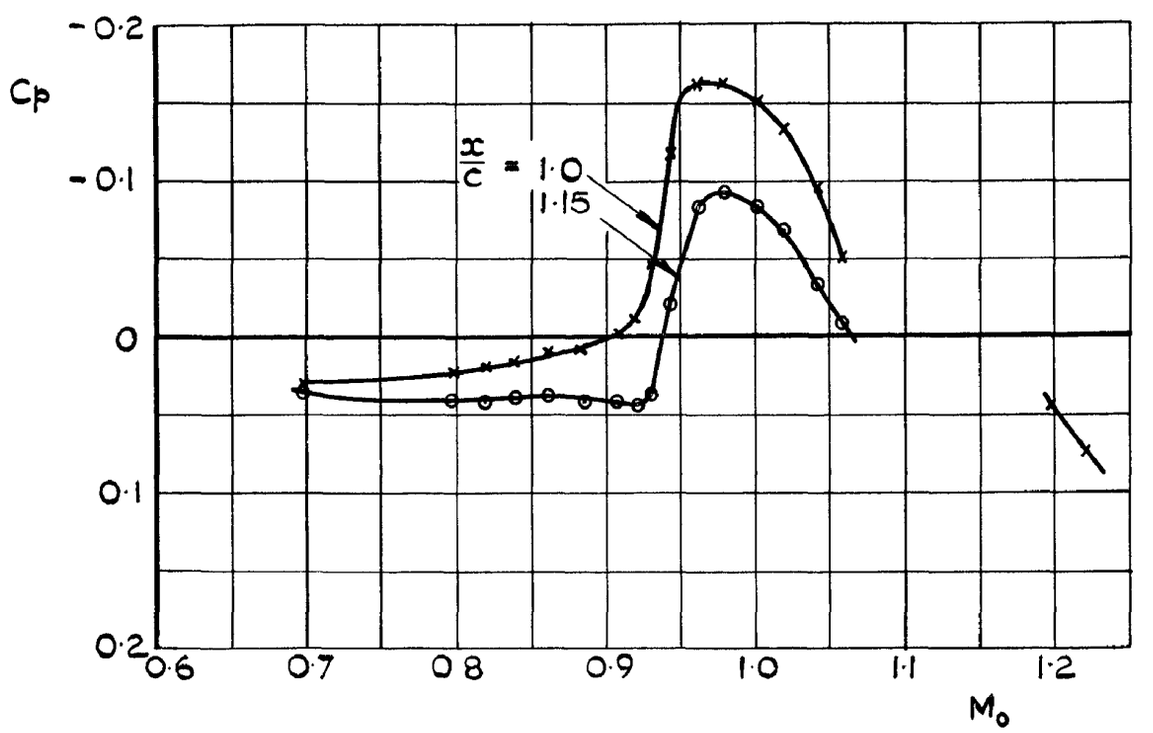

FIG. 6. VARIATION OF PRESSURE ON BODY SIDE ℄ BEHIND WING WITH FREE STREAM MACH NUMBER. (TRANSITION FIXED) (SEE PARA. 5.1.1)

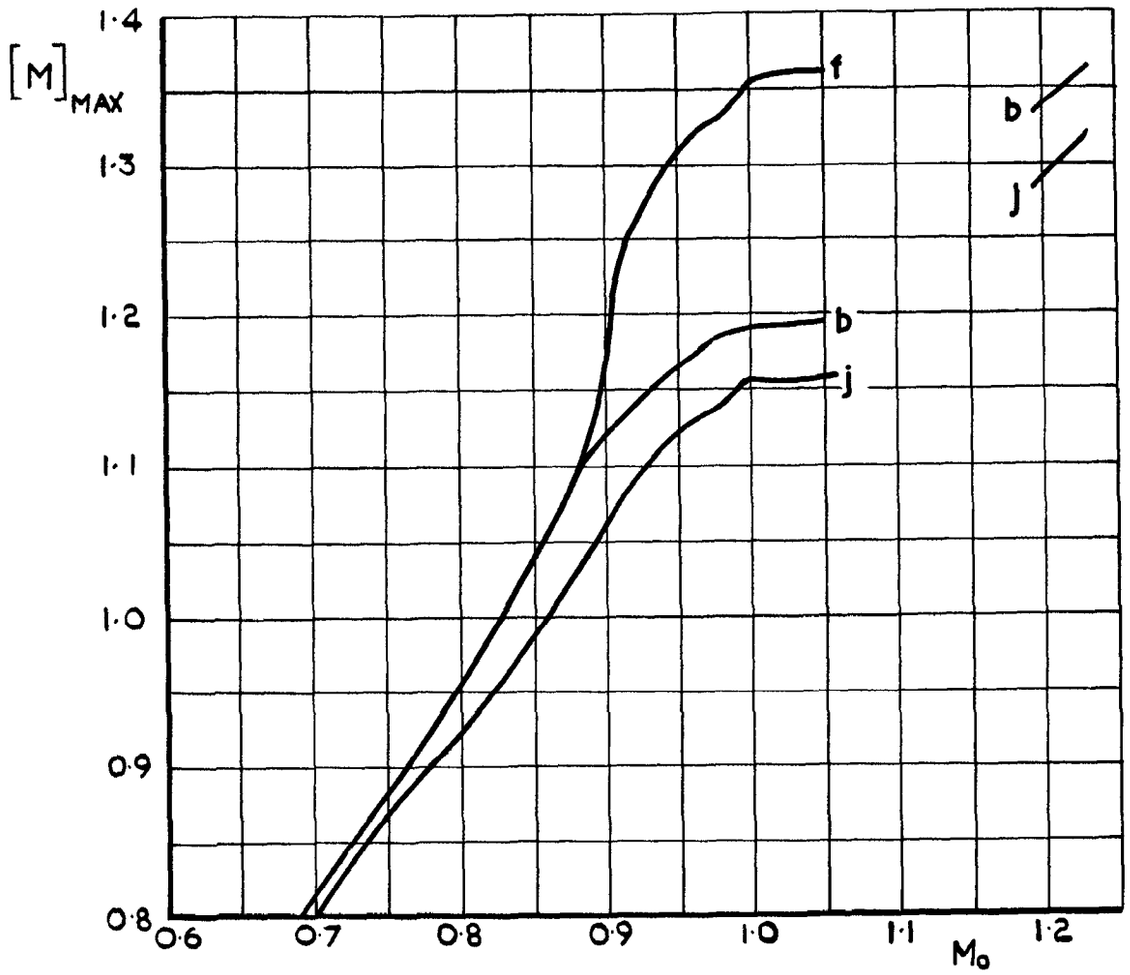

FIG 7. PEAK LOCAL MACH NUMBERS FOR SECTIONS b, f AND j (SEE PARA. 5.1)

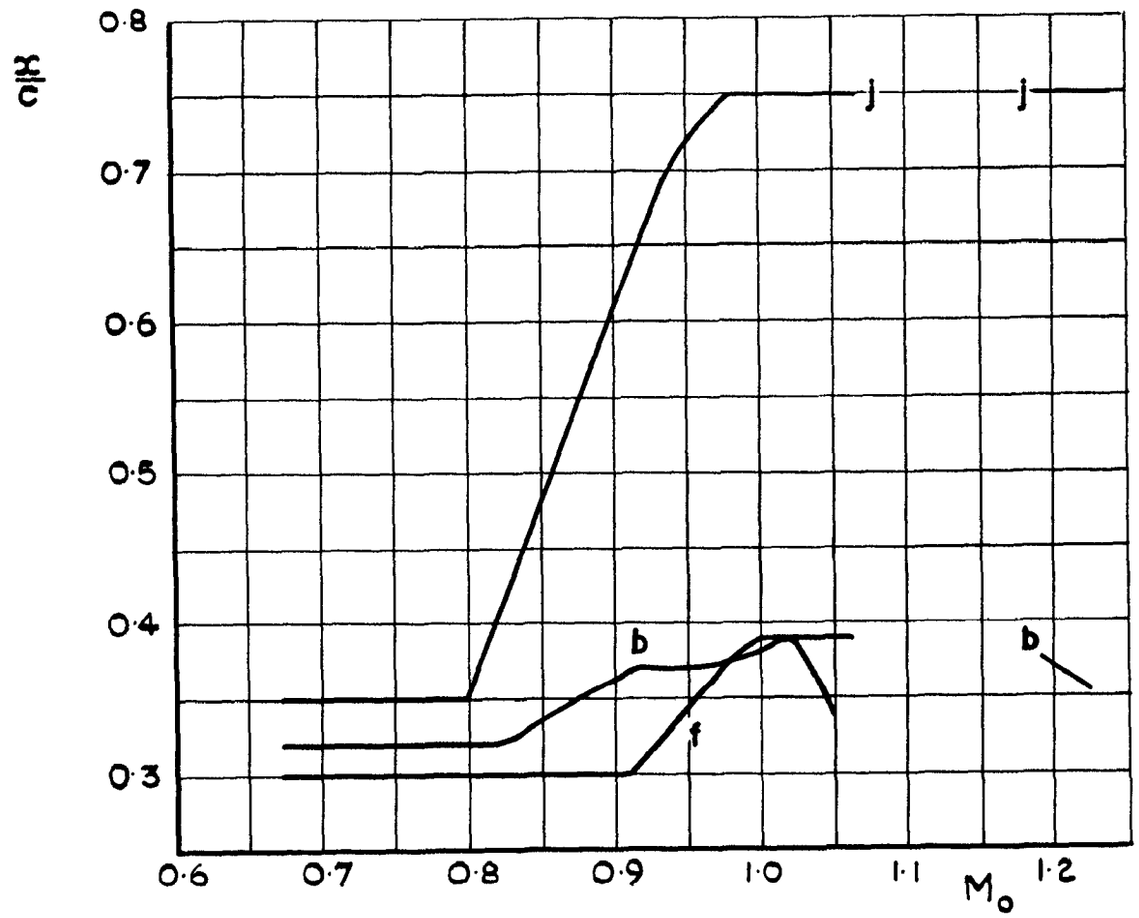

FIG. 8. POSITION OF MACH NUMBER PEAK FOR SECTIONS b, f AND j (SEE PARA 5.1.)

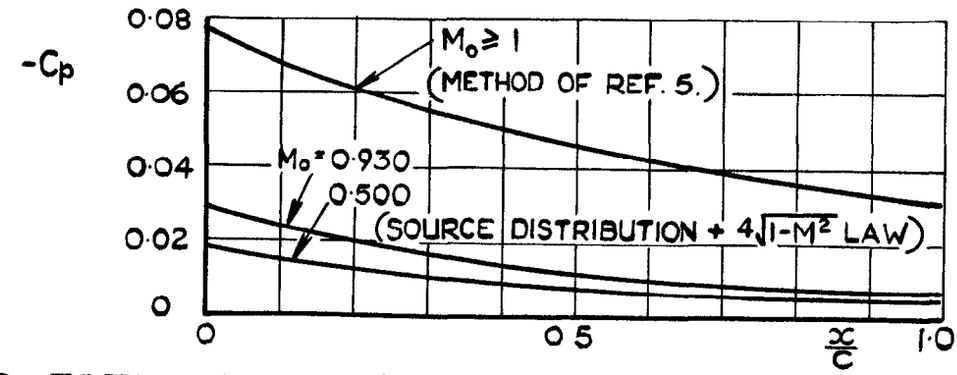

FIG. 9. ESTIMATED Cp DISTRIBUTION IN WING–BODY JUNCTION DUE TO BODY NOSE SHAPE. (SEE PARA 5.1.2.)

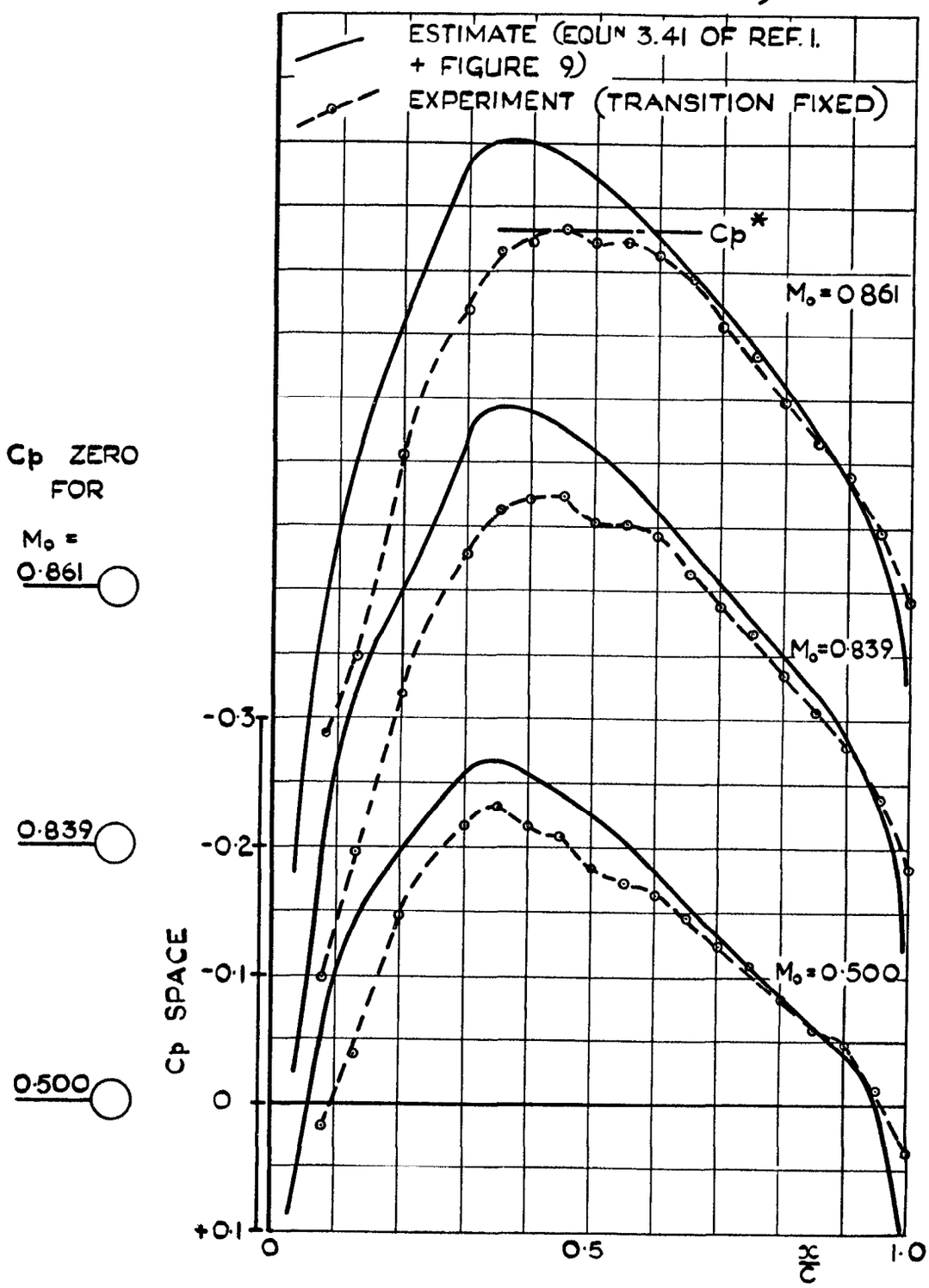

FIG. 10. COMPARISON BETWEEN ESTIMATED AND MEASURED Cp DISTRIBUTION IN WING–BODY JUNCTION (SUBSONIC) (SEE PARA 5.1.2.)

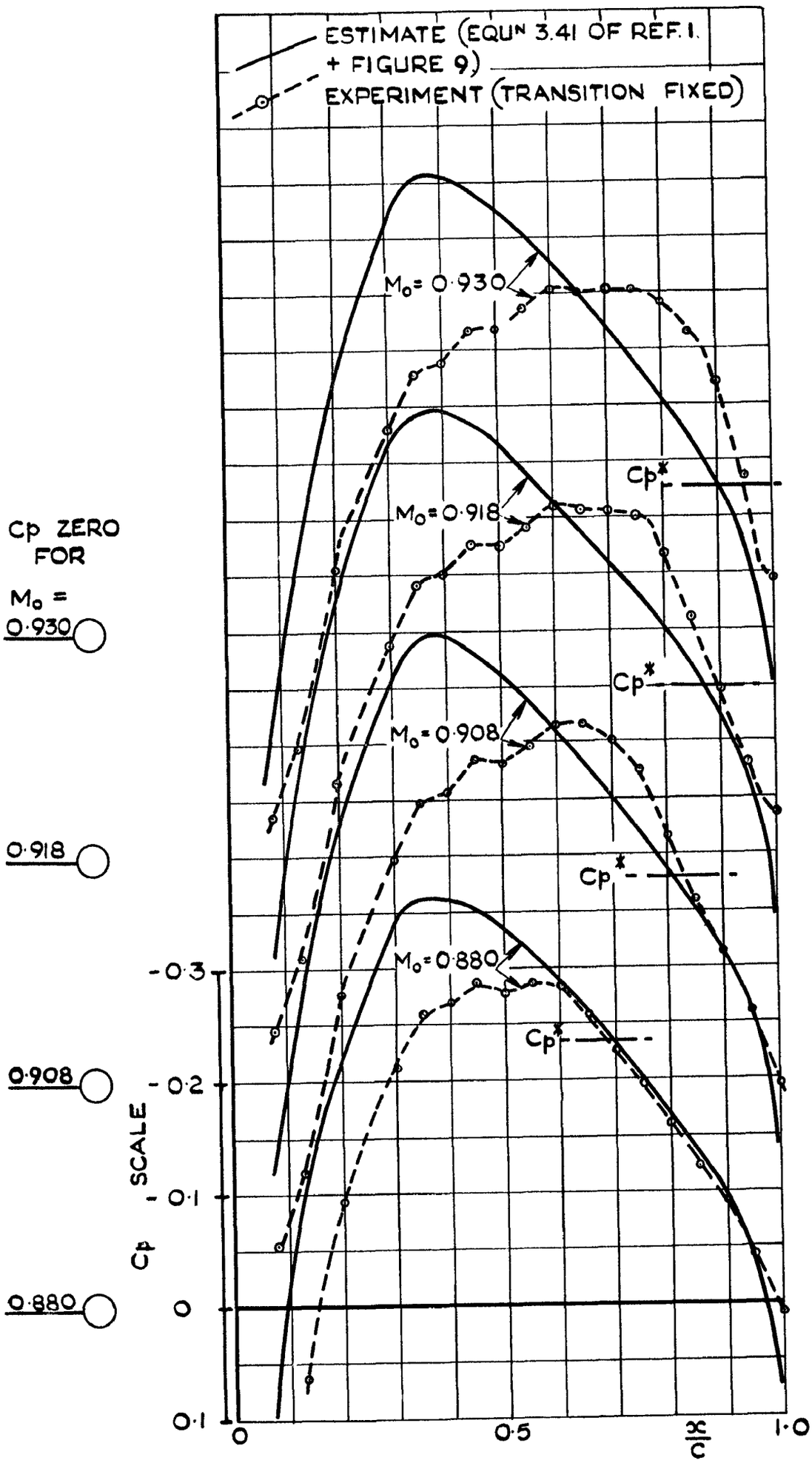

FIG. 10. CONCLUDED

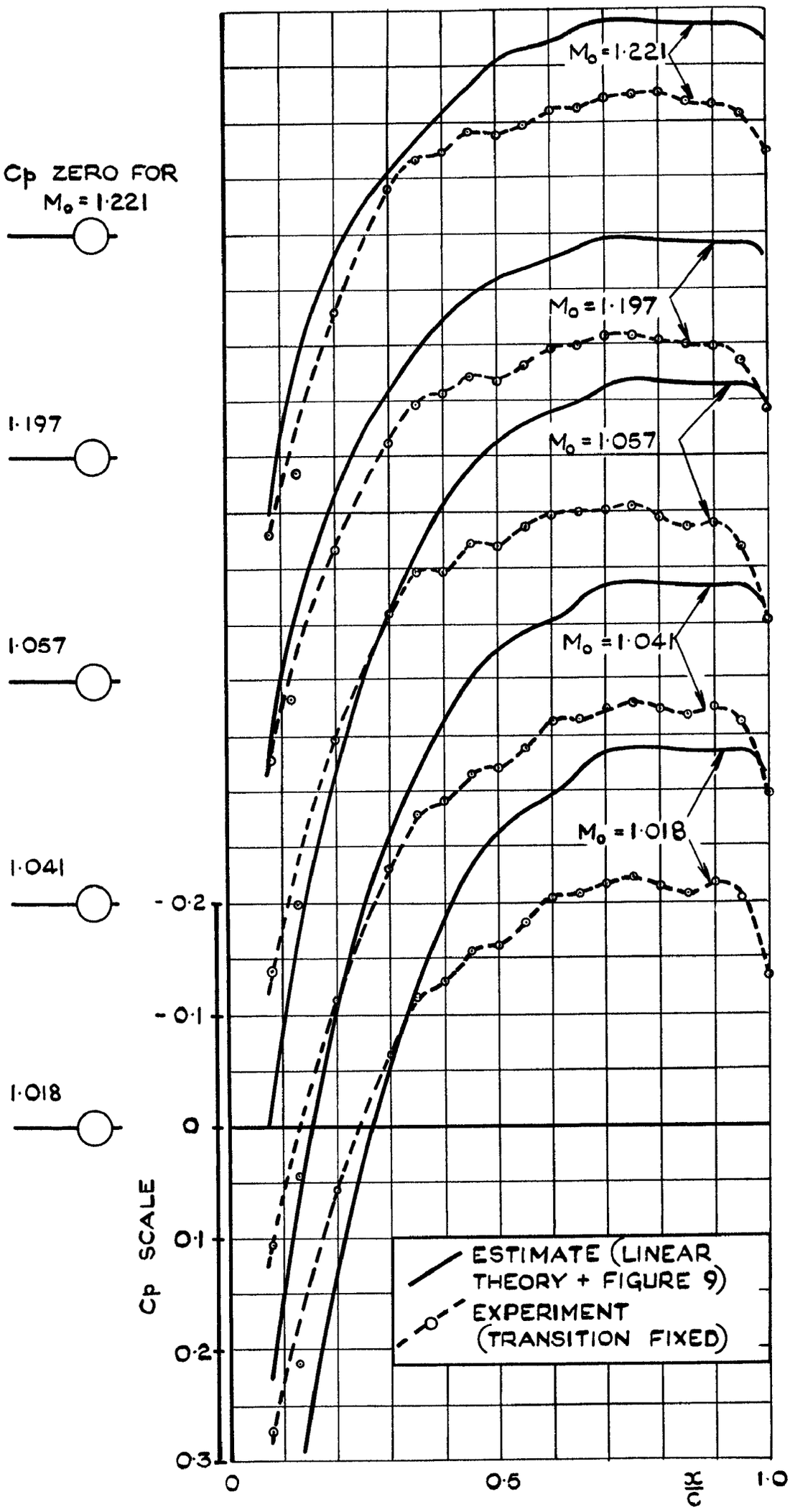

FIG. 11. COMPARISON BETWEEN ESTIMATED AND MEASURED Cp DISTRIBUTION IN WING-BODY JUNCTION (SUPERSONIC) (SEE PARA. 5.1.2)

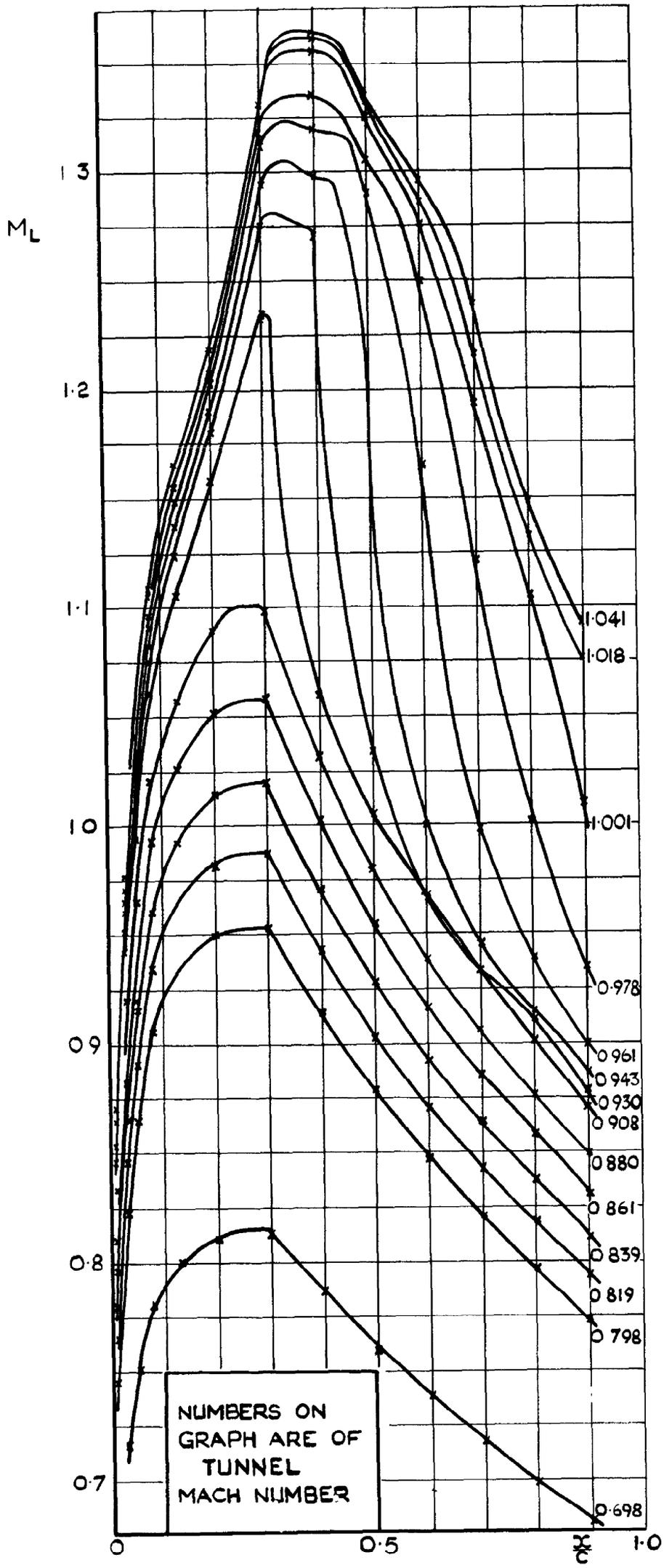

FIG. 12. LOCAL MACH NUMBER DISTRIBUTIONS SECTION f. TRANSITION FIXED (SEE PARA 5.2)

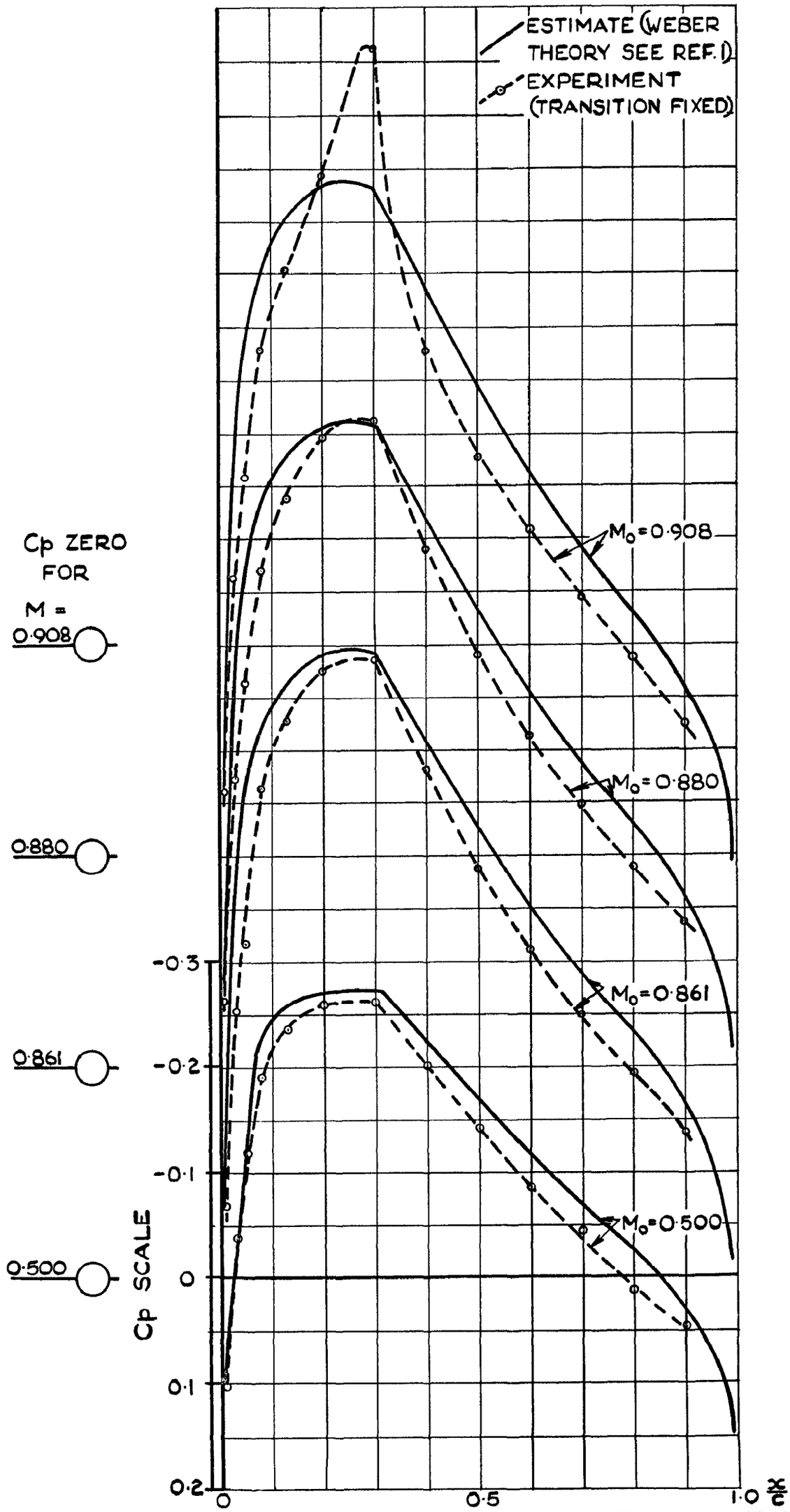

FIG. 13. COMPARISON BETWEEN ESTIMATED AND MEASURED Cp DISTRIBUTION SECTION f (TRANSITION FIXED) (SEE PARA 5.2)

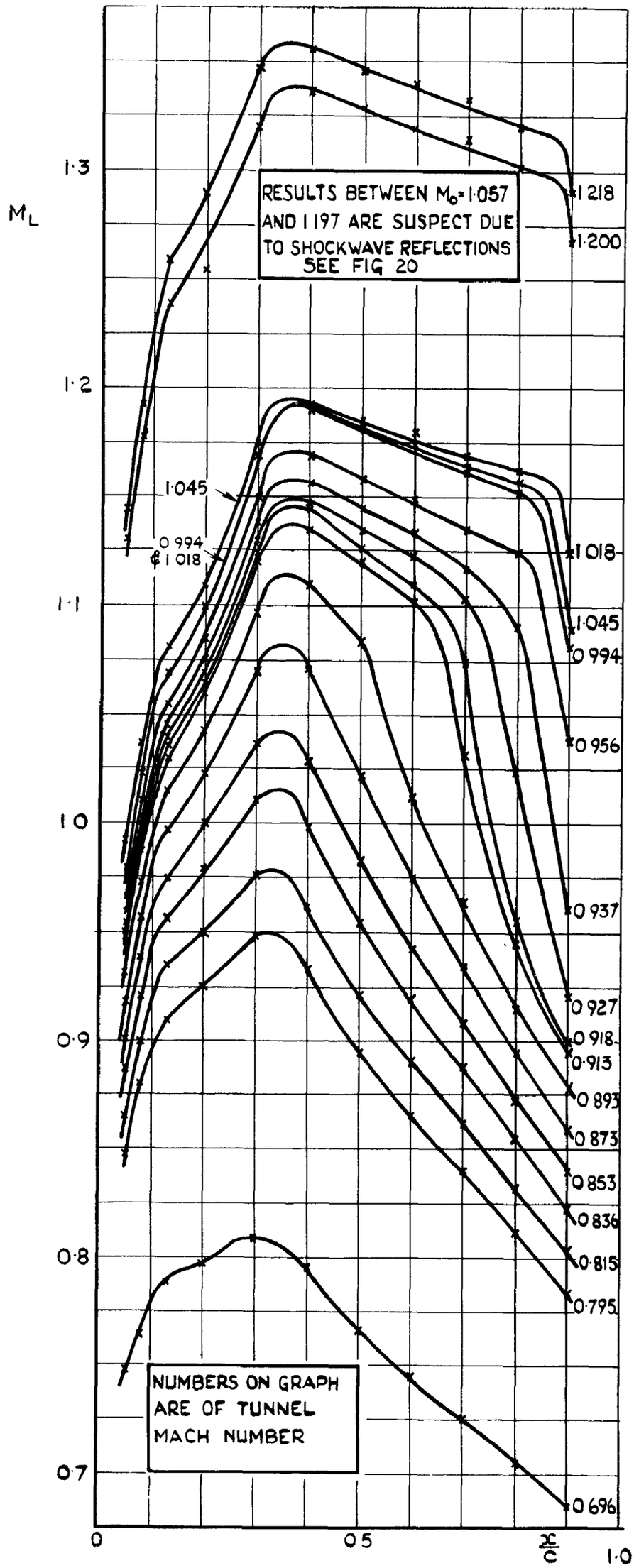

FIG. 14. LOCAL MACH NUMBER DISTRIBUTION SECTION b, NATURAL TRANSITION. (SEE PARA. 5.3).

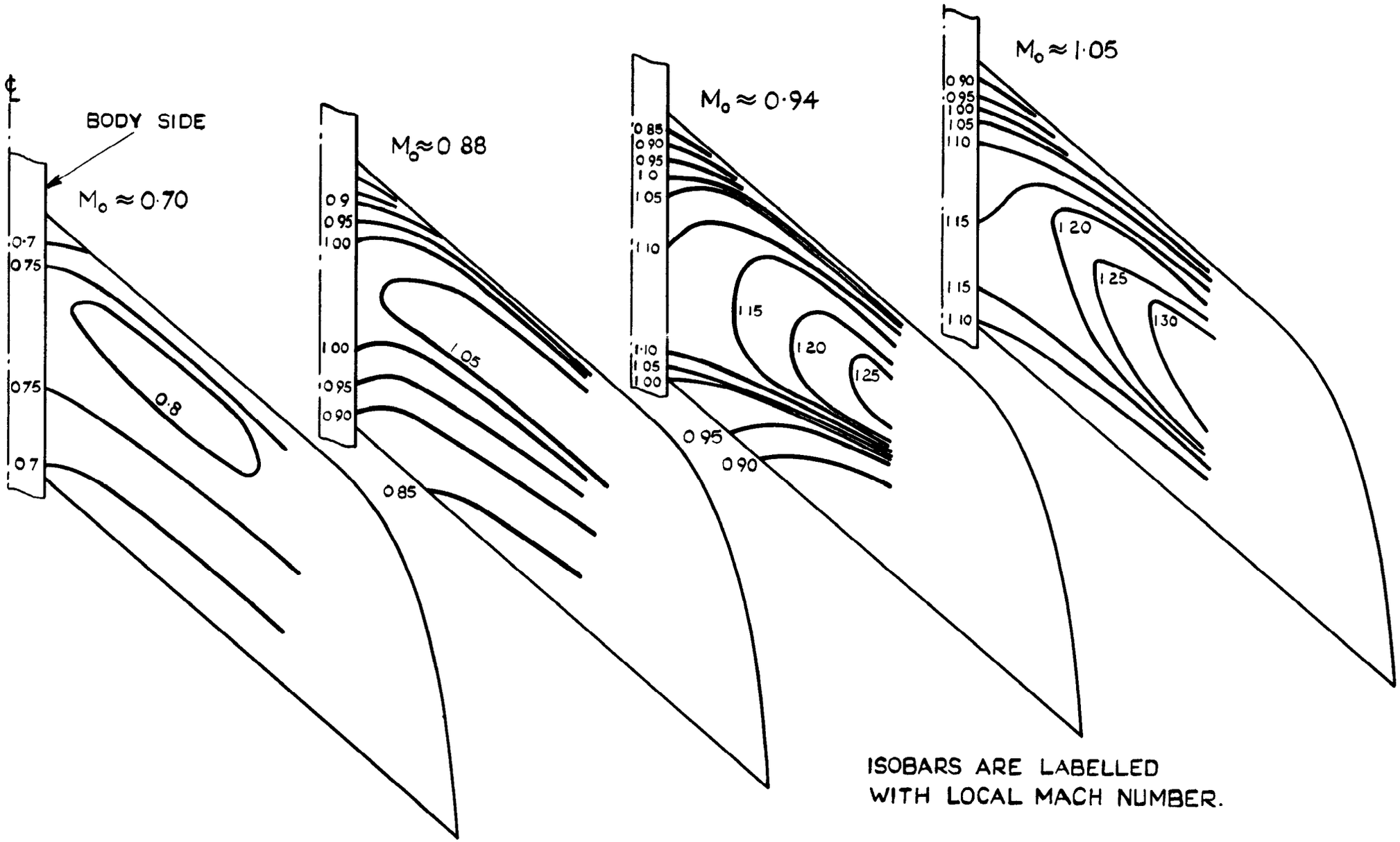

FIG. 15. ISOBAR PATTERNS ON WING WITH NATURAL TRANSITION. (SEE PARA 5.4)

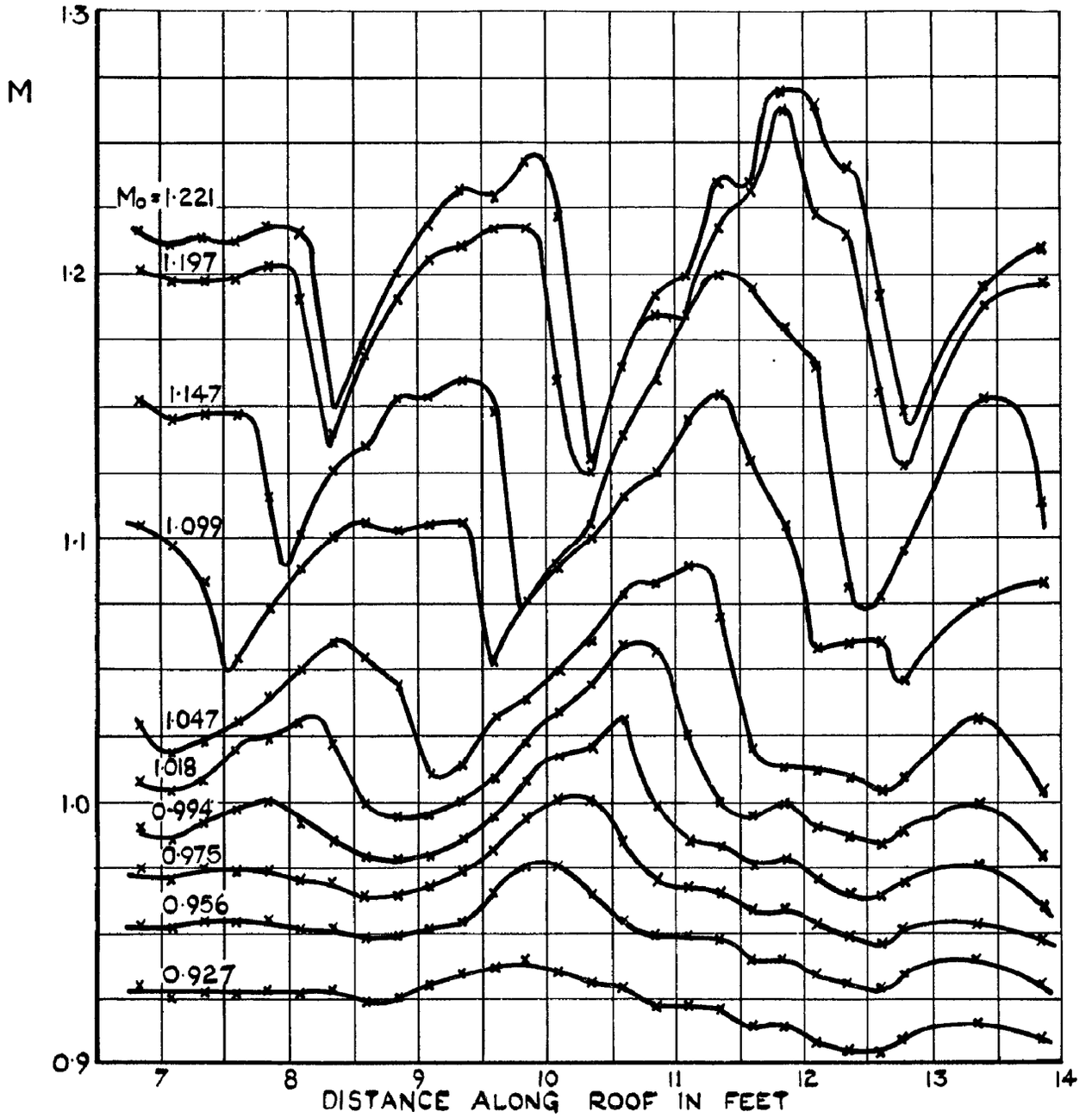

FIG. 16. MACH NUMBER DISTRIBUTION ON TUNNEL ROOF (SEE APPENDIX).

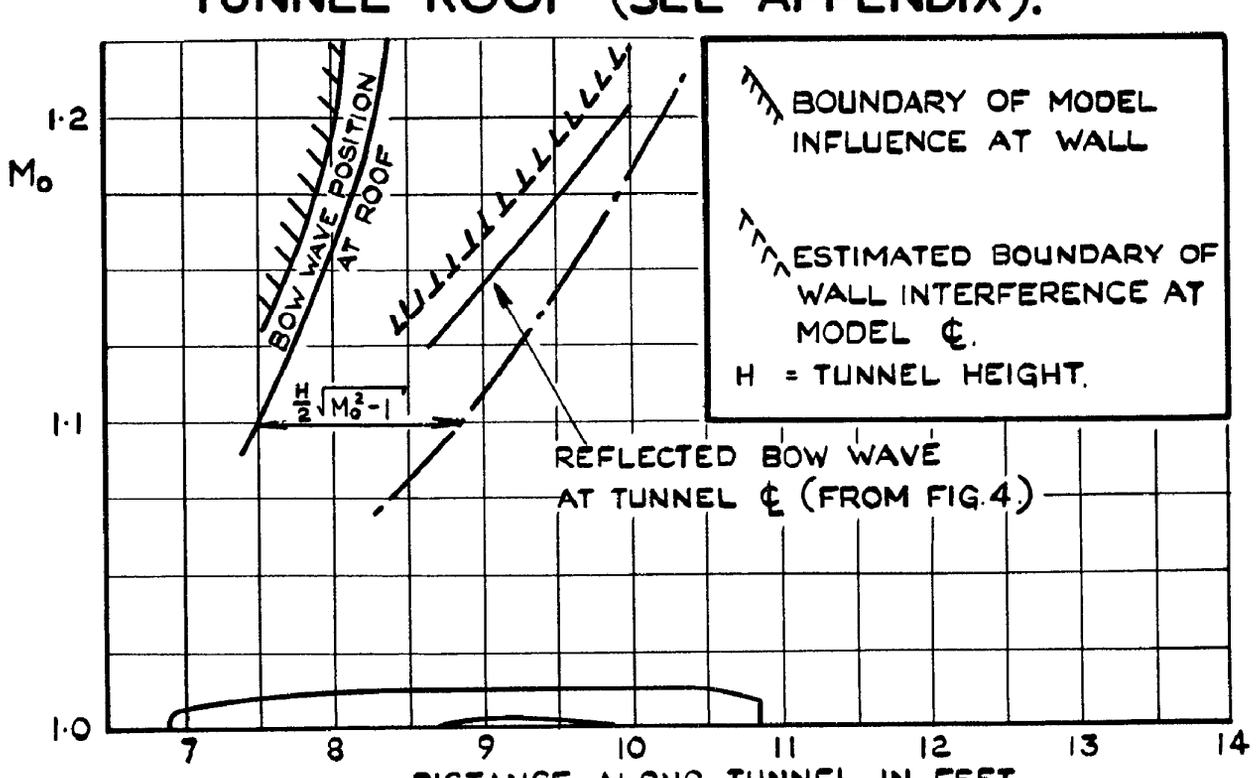

FIG. 17. ESTIMATED INTERFERENCE BOUNDARIES. (SEE APPENDIX)

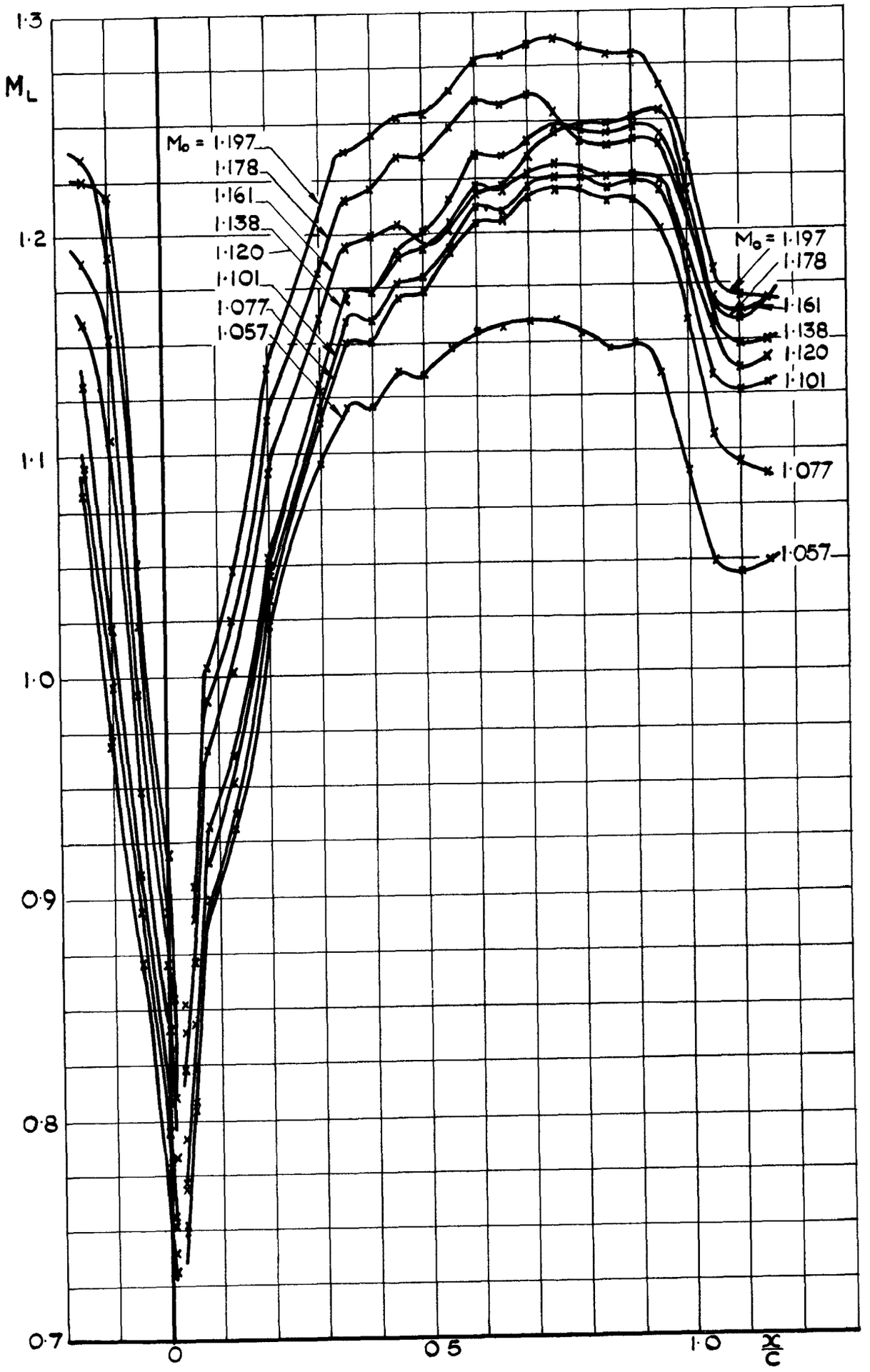

FIG. 18. LOCAL MACH NUMBER DISTRIBUTIONS IN WING-BODY JUNCTION. TRANSITION FIXED. SUSPECT RESULTS. (SEE APPENDIX)

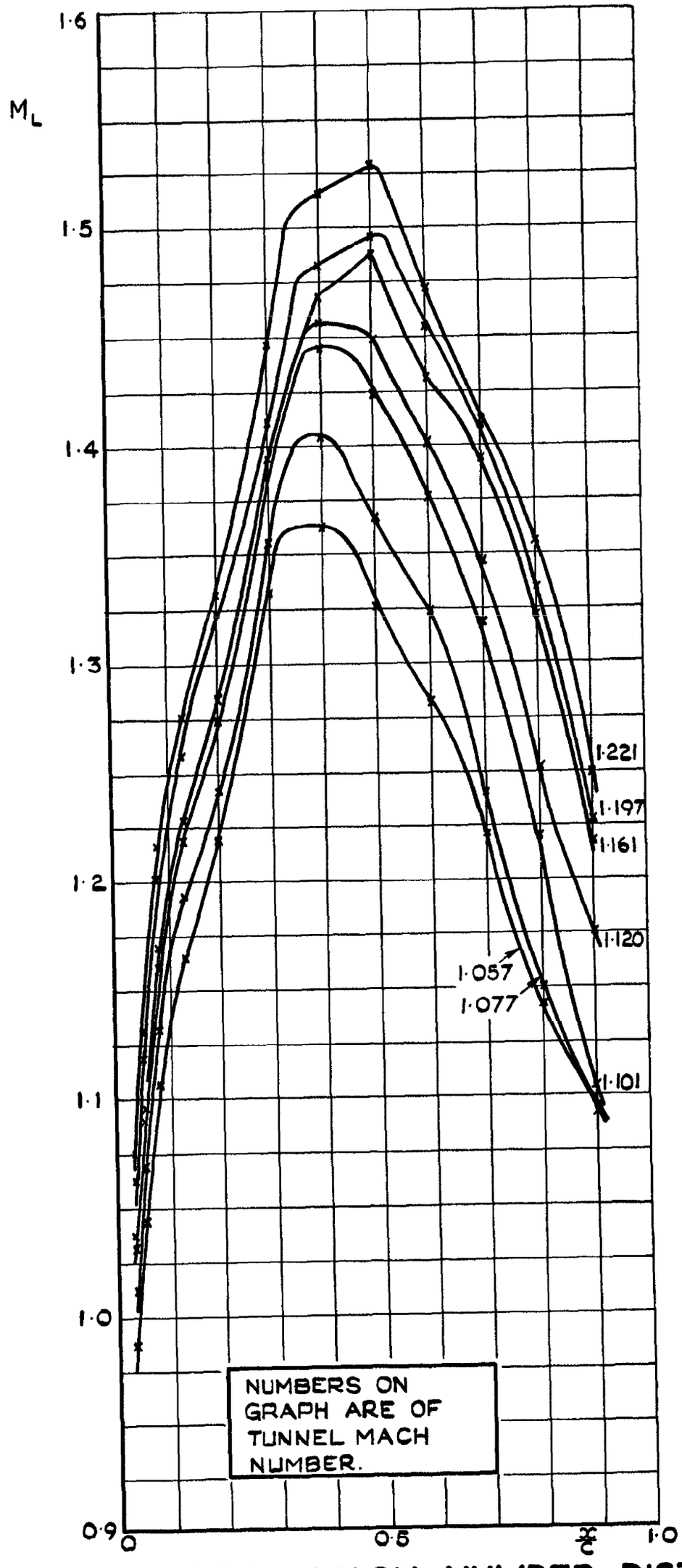

FIG. 19. LOCAL MACH NUMBER DISTRIBUTIONS SECTION f TRANSITION FIXED. SUSPECT RESULTS (SEE APPENDIX)

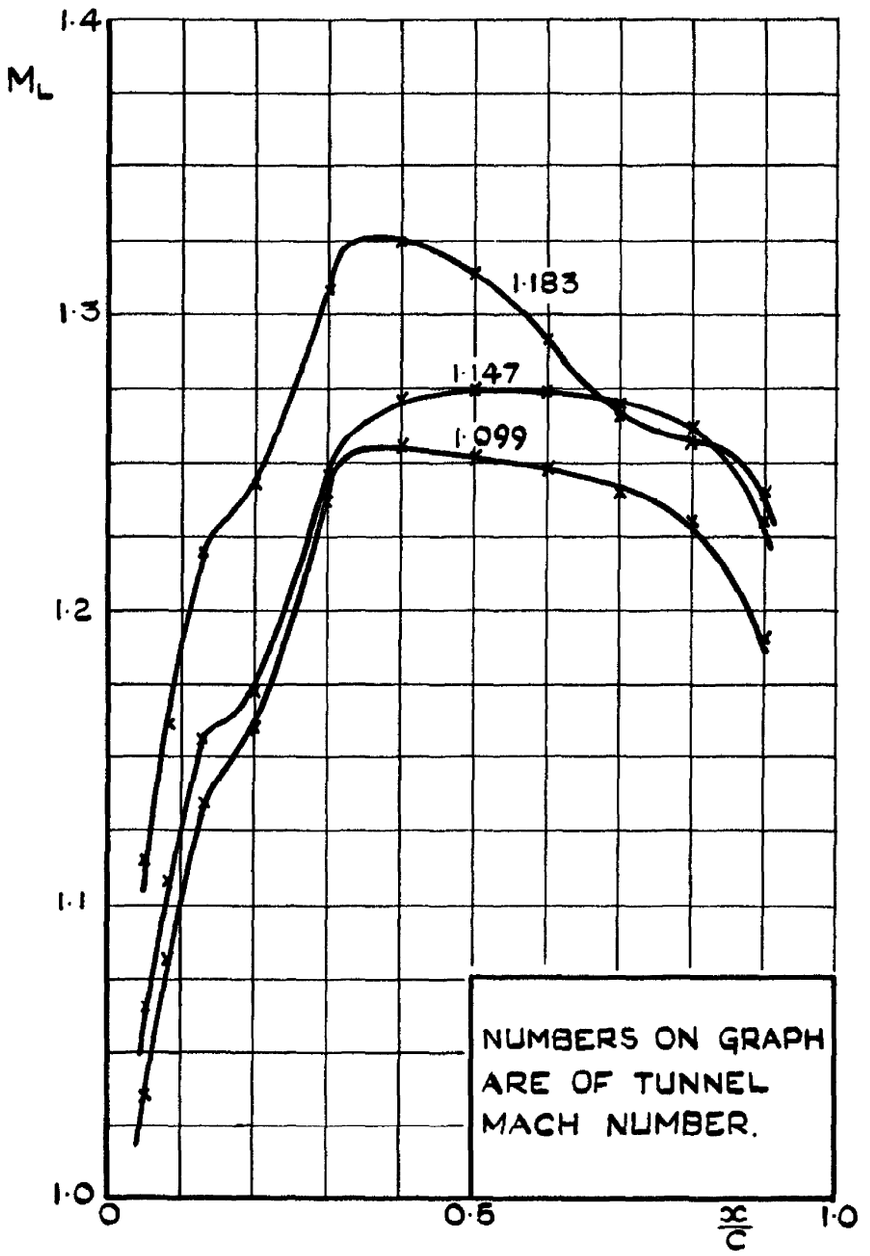

FIG. 20. LOCAL MACH NUMBER DISTRIBUTION SECTION b. NATURAL TRANSITION. SUSPECT RESULTS. (SEE APPENDIX)

A.R.C. C.P. No.542

533.693.1:
533.69.048.2:
533.6.011.35

PRESSURE MEASUREMENTS AT THE CENTRE OF A 40° SWEPT BACK WING WITH R.A.E. 101-10 SECTIONS AT ZERO INCIDENCE AND TRANSONIC SPEEDS. Rossiter, J.E. June, 1959.

Pressure distributions have been measured on a 40° swept back wing with 10% thick R.A.E. 101 sections in combination with a rectangular section body.

The range of investigation included speeds from M_0 = 0.5 to 1.22 at zero wing incidence at a Reynolds number of 1.3 million based on the wing chord. For some of the tests, boundary layer transition was fixed ahead of the 10% chord line on the wing.

Between Mach numbers of 0.88 and 0.94 the pressure distribution in the wing-body junction changed from subsonic to one having the shape associated

(Over)

A.R.C. C.P. No.542

533.693.1:
533.69.048.2:
533.6.011.35

PRESSURE MEASUREMENTS AT THE CENTRE OF A 40° SWEPT BACK WING WITH R.A.E. 101-10 SECTIONS AT ZERO INCIDENCE AND TRANSONIC SPEEDS. Rossiter, J.E. June, 1959.

Pressure distributions have been measured on a 40° swept back wing with 10% thick R.A.E. 101 sections in combination with a rectangular section body.

The range of investigation included speeds from M_0 = 0.5 to 1.22 at zero wing incidence at a Reynolds number of 1.3 million based on the wing chord. For some of the tests, boundary layer transition was fixed ahead of the 10% chord line on the wing.

Between Mach numbers of 0.88 and 0.94 the pressure distribution in the wing-body junction changed from subsonic to one having the shape associated

(Over)

A.R.C. C.P. No.542

533.693.1:
533.69.048.2:
533.6.011.35

PRESSURE MEASUREMENTS AT THE CENTRE OF A 40° SWEPT BACK WING WITH R.A.E. 101-10 SECTIONS AT ZERO INCIDENCE AND TRANSONIC SPEEDS. Rossiter, J.E. June, 1959.

Pressure distributions have been measured on a 40° swept back wing with 10% thick R.A.E. 101 sections in combination with a rectangular section body.

The range of investigation included speeds from M_0 = 0.5 to 1.22 at zero wing incidence at a Reynolds number of 1.3 million based on the wing chord. For some of the tests, boundary layer transition was fixed ahead of the 10% chord line on the wing.

Between Mach numbers of 0.88 and 0.94 the pressure distribution in the wing-body junction changed from subsonic to one having the shape associated

(Over)

with the flow at a supersonic free stream Mach number.

At subsonic speeds agreement between the measured pressure distribution in the wing body junctions and an estimate made by the method given by Küchemann and Weber was only fair mainly because the body side does not act as a true reflection plane.

At supersonic speeds, the method given by Bagley for estimating the pressure distribution at the centre section, gives the correct shape for the distribution at Mach numbers as low as 1.02 but the magnitude is in error, particularly over the rear of the section. Agreement between estimated and measured values improves as Mach number is increased but is only fair at the highest test Mach number, $M_0 = 1.22$.

with the flow at a supersonic free stream Mach number.

At subsonic speeds agreement between the measured pressure distribution in the wing body junctions and an estimate made by the method given by Küchemann and Weber was only fair mainly because the body side does not act as a true reflection plane.

At supersonic speeds, the method given by Bagley for estimating the pressure distribution at the centre section, gives the correct shape for the distribution at Mach numbers as low as 1.02 but the magnitude is in error, particularly over the rear of the section. Agreement between estimated and measured values improves as Mach number is increased but is only fair at the highest test Mach number, $M_0 = 1.22$.

Published by
HER MAJESTY'S STATIONERY OFFICE

To be purchased from
York House, Kingsway, London W.C.2
423 Oxford Street, London W.1
13A Castle Street, Edinburgh 2
109 St. Mary Street, Cardiff
39 King Street, Manchester 2
50 Fairfax Street, Bristol 1
2 Edmund Street, Birmingham 3
80 Chichester Street, Belfast 1
or through any bookseller

Printed in England

S.O. CODE No.23-9012-42